19th Brazilian Congress of Thermal Sciences and Engineering
November 06th-10th, 2022, Bento Gonçalves - RS - Brazil

ENC-2022-0061
MEASUREMENT OF REGRESSION RATE IN HYBRID ROCKET USING COMBUSTION CHAMBER PRESSURE

Isabel Pacheco Brasil de Matos
Instituto Tecnológico de Aeronáutica, 12228-900 São José dos Campos, Brazil
isabelbrasildematos@gmail.com

Leonardo Henrique Gouvêa
Instituto Tecnológico de Aeronáutica, 12228-900 São José dos Campos, Brazil
gouvea@ita.br

Pedro Teixeira Lacava
Instituto Tecnológico de Aeronáutica, 12228-900 São José dos Campos, Brazil
placava@ita.br

Abstract. *Hybrid rocket motors (HRM) never attained mainstream adoption due to its inherently low fuel regression rate, that limits its applications in relatively lower thrust levels rocket motors. The low thrust is a consequence of the difficulty in quickly mixing the fuel and oxidizer, which is characterized by a low rate of regression of the fuel grain. Therefore, the measurement of this parameter is of great importance in studies that aim solutions for this deficiency in HRM. Several studies evaluate the average regression rate over time, measuring the total mass of fuel before and after a burn (weight loss method). An alternative method to measure instantaneous regression rate was tested in this work. Using a laboratory scale test bench with high-density polyethylene (HDPE) and gaseous oxygen, the objective of this work was to develop an algorithm to determine the regression rate of a hybrid fuel by using its measured combustion chamber pressure. In this method, the choked flow condition at the nozzle throat of the hybrid rocket was used to obtain the mass of fuel burnt, and in turn the regression rate. The results obtained were compared favourably with the results from the weight loss method, proving that the algorithm developed is a reliable one.*

Keywords: *Aerospace engineering, hybrid rocket propulsion, regression rate, hybrid rocket motor, test bench.*

1. INTRODUCTION

Propulsion systems provide a force that moves bodies that are initially at rest, changes a velocity, or overcomes retarding forces when a body is propelled through a medium. Jet propulsion is a means of locomotion whereby a reaction force is impaired to a device by the momentum of ejected matter. Rocket propulsion is a class of jet propulsion that produces thrust by ejecting stored matter, called the propellant (Sutton; Biblarz, 2001). Chemical propulsion is the energy source most useful in rocket propulsion, which originates from the direct conversion of the chemical energy of the constituents of the propellant into kinetic energy through combustion and expansion processes. Depending on the physical state of the propellants, rocket propulsion can be classified as liquid, solid or hybrid (Dos Santos; Lacava, 2014).

In solid rockets, the propellant to be burned is stored in the combustion chamber, and contains all the chemical elements for complete burning, and in liquid rockets, the liquid propellants are fed under pressure from tanks into the thrust chamber (Sutton; Biblarz, 2001). Hybrid rocket motor (HRM) most commonly employ a liquid or gaseous oxidizer and a solid fuel. They provide an attractive alternative when compared to the conventional liquid or solid rockets (Kuo; Chiaverini, 2007). Compared to liquid rockets, hybrids have less complexity and lower costs, due to less piping and valves (Kobald et al., 2017). And compared to solid rockets, they have controllable thrust, shutoff and restart capability, and are safer, since the fuel is inert and can be manufactured, transported, and handled safely, avoiding the explosiveness of the solid (Kuo; Chiaverini, 2007).

In a HRM, when the fuel grain is ignited by a source of heat, the oxidizer flow provides the required flame to spread and fully ignite the motor. The mixture burns as a macroscopic turbulent diffusion flame where the oxidizer-to-fuel ratio (O/F) varies down the length of the chamber, ending at a composition that determines the motor performance (Sutton, 2001). The fuel mass flow rate depends on the fuel regression rate, which is controlled by a diffusion-limited combustion mode such that gasified fuel and oxidizer mix and burn in a turbulent boundary layer formed along the fuel surface (Ito, 2019), as seen in Fig. 1. Marxman et al. (1963, 1964) demonstrated how this phenomenon occurs in their works.

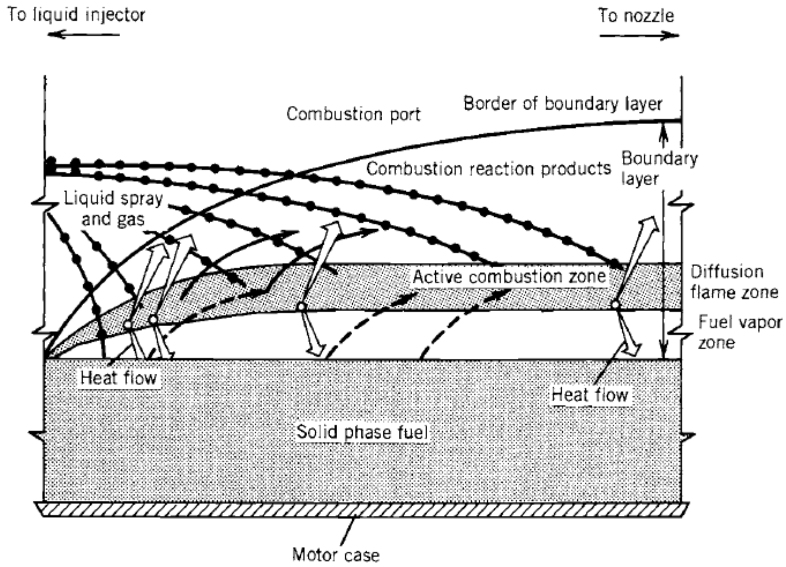

Figure 1: Simplified model of the diffusion-controlled hybrid combustion process, illustrating the flame zone embedded within the fuel boundary layer (Sutton; Biblarz, 2001).

The regression rate, or the spatially averaged burning rate of the solid fuel grain, is the most significant characterization parameter of a hybrid rocket motor, and it depends on several parameters, such as the oxidizer mass flux, chamber pressure, and axial distance along the grain (De Zilwa et al., 2004). The measurement of the regression rate can be carried out in various forms, and the most traditional is according to the weight loss method (George et al., 2001). This method uses the end-point technique, and consists in determining a time and space averaged value for the mass lost from the grain, over the duration of the burn, with corrections for the ignition and shut down transients. The drawback of this method is that, to get a complete trend line of regression rate versus oxidizer mass flux, a series of experiments need to be carried out (Kumar; Ramakrishna, 2014).

Other alternative methods have been conceived by researchers to obtain the regression rate of a hybrid fuel, which are simpler and more accurate. Time-resolved measurement of regression rate is desirable and can minimize the uncertainties associated with the ignition and shutdown transients. A time-resolved measurement provide means for obtaining multiple data points from a single test, thus, reducing the time and cost involved with testing (De Zilwa et al., 2004), and it can be obtained by measuring the instantaneous thickness or port diameter with ultrasound (Chiaverini et al., 2000; Sorge; Carmicino, 2002) or with x-ray radiography (Chiaverini et al., 2000; Evans et al., 2003b), for example. These techniques have the potential to provide real-time measurements but require specialized and expensive instrumentation (De Zilwa et al., 2004).

In this work, a simplified method to obtain the time-resolved measurement of the regression rate used by Kumar (2014), Osmon (1966), Wernmont (1999) and George (2001) is implemented. This method uses the combustion chamber pressure to obtain the regression rate of the fuel. It has advantage over the weight loss method such that in a single experiment, it can give the complete trend line of regression rate vs oxidizer mass flux.

The method studied in this work was first used by Osmon (1966), to obtain the regression rate of lithium aluminum hydrid fuel, using a motor of length 500 mm. The characteristic velocity C^* used by him was an averaged value for the entire burn time, but in an actual case it changes with burn time as the O/F ratio changes. Wernmont (1999) used a method similar to the one used by Osmon (1966) to get the regression rate of polyethylene fuel. He attempted to compute the variation of C^* with burn time by assuming a linear change in throat area with burn time. The regression rate obtained by him does not follow any trend line and he even observed a decrease in regression rate with the increase in oxidizer mass flux. George et al. (2001) used this method to obtain the regression rate of hydroxyl terminated polybutadiene (HTPB) based fuel. Their algorithm is an improvement over that used by Osmon (1966), in which they account for the variation in O/F ratio with burn time by calculating the C^*_{theo} based on the instantaneous value of O/F. They also have taken the additional care of matching the mass loss of fuel obtained from their calculation with those experimentally obtained at the end of combustion (Kumar; Ramakrishna, 2014).

The objective of this work is to determine the regression rate using combustion chamber pressure for a high regression rate fuel, where C^* changes due to the variation of O/F ratio with burn time. It is possible that the L^* (due to increase in chamber volume with burn time) also varies significantly with burn time. These results were further compared with the regression rates obtained with the weight loss method using the same motor, fuel and oxidizer combination. The high regression rate fuel used is high-density polyethylene (HDPE), and commercially available gaseous oxygen was used as the oxidizer.

2. TEST BENCH

The hybrid rocket test bench used in this work is part of LCPE (Laboratório de Combustão, Propulsão e Energia), located at ITA (Instituto Tecnológico de Aeronáutica). This motor was designed by Quadros (2017) based on experience with two previous generations of hybrid motors at LCPE (Dos Santos (2014), Barros (2014) and Dias (2015)). These early experiments used paraffin and gaseous oxygen as propellents.

Previously work by Silveira (2020) validated a theoretical simulation procedure through tests that showed that the test bench at LCPE can be used with other fuel blends, different from the one previously used. Results were obtained by comparing paraffin wax, HDPE and HTPB, and they showed that the theoretical simulation values were compatible with measured chamber pressure and thrust obtained through tests. The constant regression rate along all the length of the propellant grains was not achieved, as predicted in the simulation. It was suggested that this assumption could be achieved as desired by decreasing effects of a recirculation zone at the post chamber, and by adding a pre chamber (Silveira et al., 2020).

As shown in Fig. 2, the workbench consists of a stainless steel hybrid rocket motor with 65 mm internal diameter and adjustable length between 135 and 265 mm, two cylinders of gaseous oxygen (GOX) (low and high pressure supply lines) and a cylinder of gaseous nitrogen (N_2) (used for purging oxygen after burning). Line pressure is regulated by a pair of manual spring loaded regulators connected to the cylinders. Two solenoid valves open and close the GOX and N_2 lines to the motor. A check valve is used to avoid mixing of the gases during operation. A rupture disk safety device, rated for 50 bar, is installed close to the injector head of the motor.

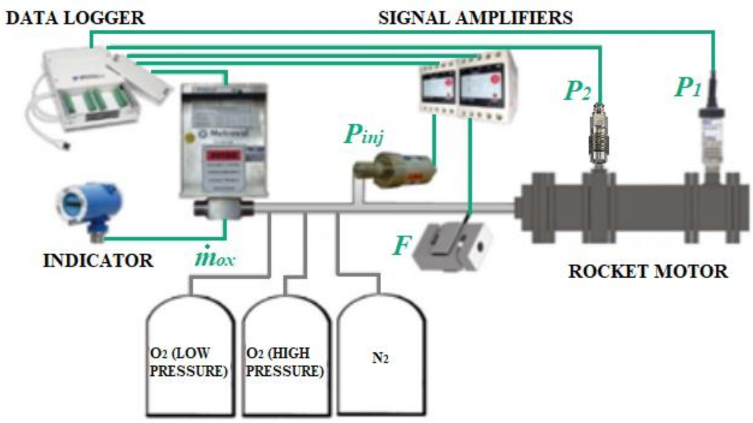

Figure 2: Parameters recorded by the data logger.

A pressure transducer (*Kyowa*, model PG-50KU), rated for up to 50 bar, is used during the test to measure GOX injection pressure. Thrust is measured by mounting the motor on a base that slides on a pair of linear guides. A load cell (*Alfa*, model SV-50) is connected to the sliding base, such that the longitudinal thrust produced compresses the cell. The 0-20 mV signals from the load cell and pressure transducer are amplified to 0-5 V by a signal conditioning unit (model MKTC-05) before reaching the data logger. Chamber pressure is measured with a piezoelectric pressure transducer (*Kistler*, model 601A), connected to the pre chamber, and with a piezoresistive strain gauge transducer (*Wika*, model S-11), rated for up to 40 bar and connected to the post chamber. The control panel commands ignition and valve opening times, according to the auto sequence set through a *LabView* program (*National Instruments*, model *USB-6259*), and receives data from the sensors at 2000 Hz.

The low pressure supply line is necessary for the ignition method used, as well as a manual controlled power source. The ignitor is made by heating a powder mixture of 65% potassium nitrate (KNO_3) and 35% Sorbitol ($C_6H_{14}O_6$) at around 120-130 °C (above the melting point of sorbitol), and casting the mixture into a cylindrical and thin desirable shape. Once cured it forms hard grains which are susceptible to moisture and mechanical impact but can otherwise be stored for several months (Olde et al., 2019). To ignite the system, the ignitor is placed inside the HDPE internal diameter, and a nickel-chromium wire is connected to one end of the ignitor, which is then attached to an electrical lead wire to a 12 V battery, used as the electrical power source.

GOX is injected with a constant mass flow rate in the combustion chamber, and hot and cold tests are made. Fig. 3 shows the combustion chamber schematics. The axial injector is a plate made of stainless steel 304, with a 4.17 mm orifice in the center. For the test studied in this work, the HDPE grain has specific mass of 960 kg/m^3, length of 150 mm, 64.90 mm of external diameter and 27.25 mm of internal diameter.

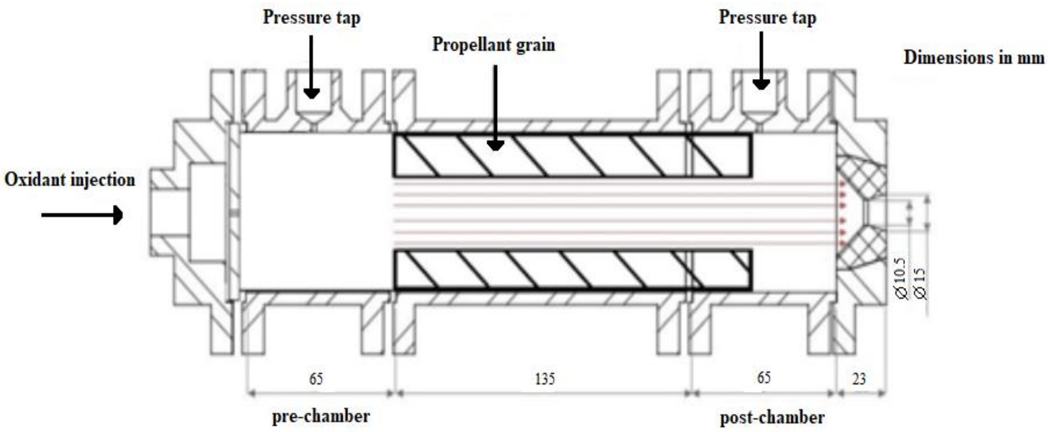

Figure 3: Combustion chamber schematics.

3. METHODOLOGY

3.1 Average regression rate measurement

Early studies on hybrid rocket motor regression characteristics generally employed average values of the regression rate based on measuring the fuel geometry or mass before and after motor firing. One way to measure the steady-state regression rate is with the time variation of the material thickness for a period of time, which should be as short as possible, depending on the spatial resolution of the method (Kuo; Chiaverini, 2007). Using experimental data, the average regression rate is calculated as shown in Eq. (1) (Gomes; Rocco; Rocco, 2015).

$$\dot{r} = \frac{D_f - D_i}{\Delta t} \quad (1)$$

Where D_f and D_i are the initial and final internal grain diameter, and Δt is the burn time. The time-space-averaged regression rate is calculated with the fuel-mass loss method in Eq. (2) (Bianchi, D.; Leccese, G.; Nasuti, F., 2017).

$$\bar{\dot{r}} = \frac{\overline{\dot{m}_f}}{\rho_s \pi \bar{D} L} \quad (2)$$

Where ρ_s is the fuel density, $\bar{D}$ is averaged port diameter, L is the length of the grain, and $\overline{\dot{m}_f}$ is the time-averaged fuel mass flow rate, determined by dividing the measured fuel mass loss ΔM by the burning time Δt, as seen in Eq. (3) (Bianchi, D.; Leccese, G.; Nasuti, F., 2017).

$$\overline{\dot{m}_f} = \Delta M / \Delta t \quad (3)$$

The averaged port diameter over the entire burning, $\bar{D} = (D_0 + \widehat{D_2})/2$, is determined with values from the initial port diameter D_0 and the final one $\widehat{D_2}$, estimated by means of the fuel mass consumed, as follows in Eq. (4) (Bianchi, D.; Leccese, G.; Nasuti, F., 2017).

$$\widehat{D_2} = \sqrt{\left(D_0{}^2 + \frac{4\Delta M}{\pi \rho_s L}\right)} \quad (4)$$

The firing test average values obtained using Eq. (1-4) are summarized in Table 1, knowing the burning time Δt is 10 seconds.

Table 1: Firing test average results, using HDPE as fuel.

Experiment no	$\dot{r}$ (mm/s)	$\bar{D}$ (mm)	$\bar{\dot{r}}$ (mm/s)	$\bar{p}_c$ (atm)	$\overline{O/F}$
1	0.3600	30.2274	0.2977	9.5516	6.3404

Assuming a uniform inner diameter growth, the average oxidizer mass flux is calculated using Eq. (5) (Gomes; Rocco; Rocco, 2015).

$$\overline{G_{ox}} = \frac{\dot{m}_{ox}}{\pi\left(\frac{D_i+D_f}{2}\right)^2} \tag{5}$$

Where $\dot{m}_{ox}$ is the oxidizer mass flow rate. Average values of the regression rate studies were utilized to develop correlations that contain the mass flux raised to an empirical power (Kuo; Chiaverini, 2007). Fuel regression rate ($\dot{r}$) in HRM is dependent on the oxidizer mass flux through the port (G_{OX}), as indicated by the empirical correlation in Eq. (6) (De Zilwa et al., 2004).

$$\dot{r} = a\, G_{ox}^{n} \tag{6}$$

Where a is the regression rate experimental coefficient incorporating grain length, G_{OX} means the average oxidizer mass flux rate and n is the experimental regression rate exponent. Previously experimental works (De Matos et al., 2021) with HDPE at the same test bench reduce Eq. (6) to a regression rate law of $\dot{r} = 0.389\, {G_{OX}}^{0.434}$. Other empirical correlations for this propellant combination found in the literature review are $a = 0.339$ and $n = 0.259$ (Gomes; Rocco; Rocco, 2015) and $a = 0.055$ and $n = 0.362$ (Carmicino, C.; Sorge, A., 2005), where fuel regression rate has units of mm/s and oxidizer mass flux has units of kg/m^2s.

3.2 Instantaneous Regression Rate Measurement using Chamber Pressure

In the method studied in this work, the relations for the chocked flow through the nozzle are used to obtain the regression rate using Eq. (7-14) presented hereafter. The mass flow rate of oxidizer $\dot{m}_{ox}$ is obtained with Eq. (7).

$$\dot{m}_{ox} = \frac{c_{ds} P_s A_{ts}}{C^*_{ox}} \tag{7}$$

Where c_{ds} is the coefficient of discharge at the exit of the settling chamber, P_s is the settling chamber pressure, A_{ts} is the throat area of nozzle at settling chamber exit, and C^*_{ox} is the characteristic velocity of oxidizer. Eq. (8) is used in order to calculate the characteristic velocity of oxidizer C^*_{ox}.

$$C^*_{ox} = \frac{1}{\Gamma_s \gamma_{ox}} \sqrt{\frac{R_u T_{ox}}{\mathrm{M}_{ox}}} \tag{8}$$

Where R_u is the universal gas constant, T_{ox} is the settling chamber temperature, M_{ox} is the molecular mass of oxidizer, and γ_{ox} is the specific heat ratio of oxidizer. The parameter Γ_s is a function of γ_{ox}, and is obtained with Eq. (9).

$$\Gamma_s(\gamma_{ox}) = \sqrt{\gamma_{ox}} \left[\frac{2}{\gamma_{ox}+1}\right]^{(\gamma_{ox}+1)/2(\gamma_{ox}-1)} \tag{9}$$

The mass flow rate of fuel $\dot{m}_f$ is obtained with Eq. (10).

$$\dot{m}_f = \frac{P_c A_t}{C^*} - \dot{m}_{ox} \tag{10}$$

Where P_c is the combustion chamber pressure, A_t is the nozzle throat area at combustion, and C^* is characteristic velocity. With Eq. (11) is possible to calculate the characteristic velocity C^*.

$$C^* = \frac{1}{\Gamma_c \gamma_p} \sqrt{\frac{R_u T_c}{\mathrm{M}_p}} \tag{11}$$

Where T_c is the combustion chamber temperature, M_p is the molecular mass of burnt product, and γ_p is the specific heat ratio of burnt product. The parameter Γ_c is a function of γ_p, and is obtained using Eq. (12).

$$\Gamma_c(\gamma_p) = \sqrt{\gamma_p} \left[\frac{2}{\gamma_p+1}\right]^{(\gamma_p+1)/2(\gamma_p-1)} \tag{12}$$

Eq. (10) is further used to calculate the regression rate $\dot{r}$ using Eq. (13).

$$\dot{r} = \frac{\dot{m}_f}{\pi \rho_f d_p L_g} \quad (13)$$

Where ρ_f is the density of fuel, d_p is the port diameter, and L_g is the fuel grain length. The oxidizer mass flux G_{ox} is calculated with Eq. (14).

$$G_{ox} = \frac{4\dot{m}_{ox}}{\pi d_p^2} \quad (14)$$

The average value of combustion efficiency is obtained using Eq. (15) and (16) (Karabeyoglu et al., 2004; Kumar; Ramakrishna, 2011). Eq. (15) calculates the experimental characteristic velocity C^*_{expt}.

$$C^*_{expt} = \frac{\bar{p}_c A_t \Delta t_o}{m_f + m_{ox}} \quad (15)$$

Where $\bar{p}_c$ is the average chamber pressure and Δt_0 is the overall time of combustion (10s). The combustion efficiency η is calculated with Eq. (16).

$$\eta = \frac{C^*_{expt}}{C^*_{theo}} \quad (16)$$

The variation of the theoretical characteristic velocity C^*_{theo} with O/F is calculated using CEA NASA tool, that calculates chemical equilibrium product concentrations from any set of reactants, as described by Gordon and Mcbride (1994). The O/F ratio was varied and the corresponding variation of C^*_{theo} is shown if Fig. 4.

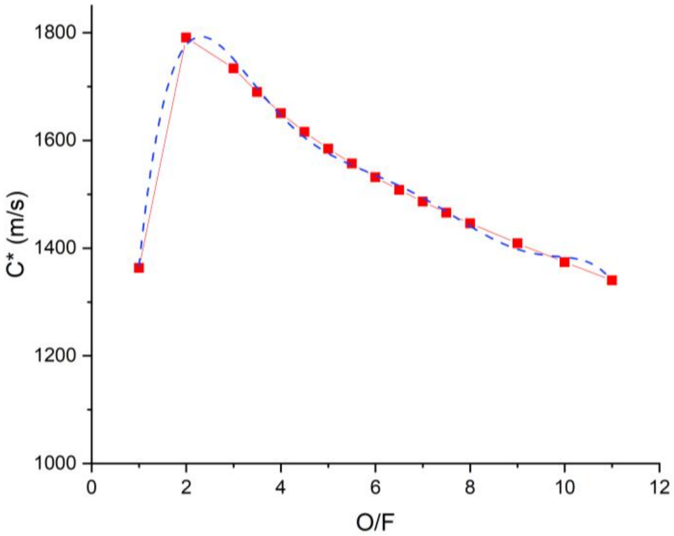

Figure 4: C^*_{theo} for varying O/F ratio, obtained from CEA NASA.

From Fig. 4 it is evident that C^*_{theo} is a function of O/F. The blue dashed line in Fig. 4 is the polynomial curve fit given by Eq. (17).

$$C^* = -0.0065(O/F)^6 + 0.367(O/F)^5 - 8.1674(O/F)^4 + 90.466(O/F)^3 - 516.74(O/F)^2 + 1373.5(O/F) + 443.36 \quad (17)$$

Next was studied the possible variation of the combustion efficiency η as a function of the characteristic length L^*. The L^* in the motor considered here changes with burn time from 1.12 m at the start of the experiments to 1.42 m at the end of the 10 s burn time. The final value of L^* is approximately 1.3 times the starting value. L^* is calculated according to Eq. (18).

$$L^* = \frac{V_c}{A_t} = \frac{\frac{\pi}{4} d_p^2 L_g}{\frac{\pi}{4} d_t^2} \quad (18)$$

Where d_t is the nozzle throat diameter. Knowing the equations previously mentioned, the following 8 steps procedure in Table 2 was adopted to obtain the regression rate vs oxidizer mass flux using combustion chamber pressure.

Table 2. Steps to obtain the regression rate vs oxidizer mass flux using combustion chamber pressure.

Step	Procedure
1	Obtain mass flow rate oxidizer $\dot{m}_{ox}(t)$ with the known settling chamber pressure P_s, average settling chamber temperature T_s, and throat area A_{ts} using Eq. (7) to (9).
2	Assume a value for the combustion efficiency η and for the equivalence ratio $\emptyset$.
3	Calculate $\dot{m}_f(t)$ knowing $\emptyset$ and $\dot{m}_{ox}(t)$.
4	With the known value of $\emptyset$ calculate C^*_{theo} from the Eq. (17).
5	Calculate the mass flow rate of fuel $\dot{m}'_f(t)$, with the known value of combustion chamber pressure $P_c(t)$, C^*_{theo} from step 4 and η from step 2, using Eq. (19). $\dot{m}'_f = \frac{P_c(t)A_t}{\eta C^*_{theo}} - \dot{m}_{ox}(t)$ (19)
6	The new O/F ratio $\emptyset'$ is calculated with the known $\dot{m}_{ox}(t)$ from step 1 and known $\dot{m}'_f(t)$ from step 5, using Eq. (20). $\emptyset'(t) = \frac{\dot{m}_{ox}(t)}{\dot{m}'_f(t)}$ (20)
7	This $\emptyset'(t)$ replaces the old $\emptyset$ of step 2 and $\dot{m}'_f(t)$ replaces $\dot{m}_f(t)$ of step 3. The process is repeated to get new $\dot{m}'_f(t)$. If $\left\|\dot{m}'_f(t) - \dot{m}_f(t)\right\| \times \Delta t \leq 5 \times 10^{-5}$ kg go to step 8. Else, change $\emptyset'(t) = \emptyset(t) - [\emptyset'(t) - \emptyset(t)] \times [\dot{m}'_f(t) - \dot{m}_f(t)]$ and go to step 3.
8	Using this $\dot{m}'_f(t)$ calculate the regression rate using Eq. (13) and G_{ox} using Eq. (14).

4. RESULTS AND DISCUSSIONS

The experiment was conducted for a burn time of 10 seconds. Chamber pressure, injection pressure, and thrust curves obtained in the test are presented in Fig. 5.

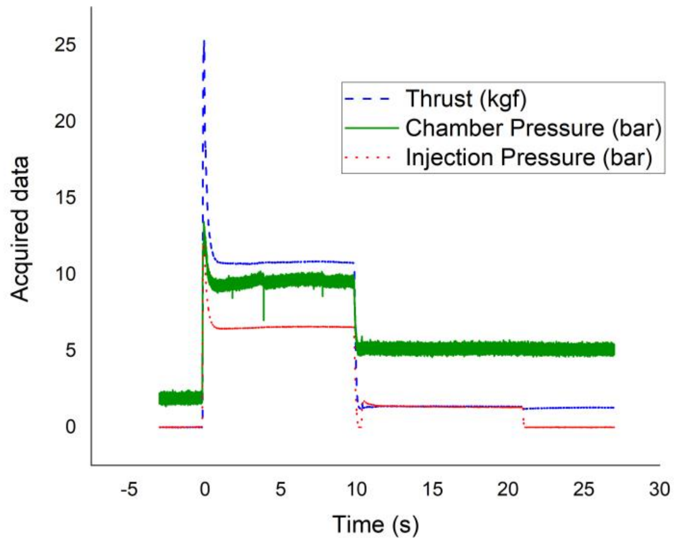

Figure 5: Curves of oxidizer feed pressure, chamber pressure and thrust.

The total mass of fuel burnt and oxidizer consumed in 10 s were also obtained, and are shown in Tab. 3.

Table 3. Total mass of fuel and oxidizer consumed in 10s.

Experiment no	Total mass of fuel consumed (g)	Total mass of oxidizer consumed (g)	Average O/F ratio	Average chamber pressure (bar)	Average thrust (kgf)
1	35	221.9	6.34	9.55	10.88

As seen in Fig. 5, during the transient period (start and stop of combustion), pressure and thrust values are lower than the average value indicated in Tab. 3. This makes it difficult to choose the exact point on the graph to analyze. In the present study, the burn time is restricted to 10 s, so the final point chosen corresponds to the stopping of the oxygen supply. Then, the initial point is chosen such that there are 20000 data points (10 s and sampling rate of 2000 kHz) between the final and initial points.

The C^*_{expt} was calculated using Eq. (15). With the known value of C^*_{expt} and C^*_{theo} obtained from CEA NASA, the η was obtained using Eq. (16). The results are shown in Fig. 6.

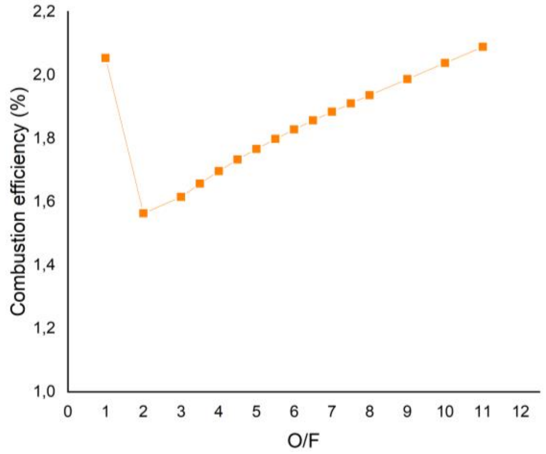

Figure 6: Relation between the η and O/F.

It is evident from Fig. 6 that the variation in combustion efficiency (η) with 10 s burn time is small. The reason for this might be that as O/F increases, L^* also increases, causing the residence time of the gases to increase as the flow velocities in the port are reduced (d_p increases). Since η is nearly constant, its averaged value of 1.84 was used in this work to determine the regression rate using combustion chamber pressure.

The regression rate obtained using the above procedure and with the weight loss method is shown in Fig. 7. The lower regression rate at lower values of G_{ox} can be due to the fact that the pressure is lower at the start of the combustion process.

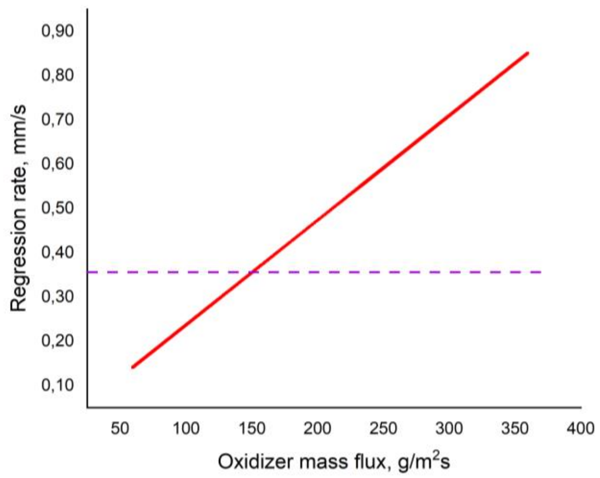

Figure 7: Regression rate obtained with pressure time graph and with weight loss method.

The value of the regression rate with the weight loss method is $0.36\ mm/s$, and is represented in Fig.7 by the dashed purple line. The regression rate obtained with the methodology presented using chamber pressure is shown by the continuous red line. It is observed from Fig. 7 that the regression rate obtained with the algorithm previously presented matches with the time and space averaged value obtained using the weight loss method.

5. CONCLUSION

This paper validated an algorithm used to determine the regression rate using pressure time trace for a hybrid rocket test bench motor using high-density polyethylene (HDPE) and gaseous oxygen. The pressure time trace was obtained from a fast response signal from a piezoelectric pressure transducer and a piezoresistive strain gauge transducer. The results obtained were compared favorably with the results found using the weight loss method for the same motor, fuel and oxidizer combination, chamber pressure and mass flow rate of oxidizer.

Given that this technique does not require any custom equipment, rather a high-speed pressure transducer that is typically an integral part of most rocket test facilities, this work can be considered of great value for measuring the regression rate at a low cost in future studies on hybrid propulsion.

6. ACKNOWLEDGEMENTS

The authors would like to thank the support of the staff of the laboratories LCPE and FENG, ITA.

7. REFERENCES

Sutton, G. P.; Biblarz, O. "Rocket Propulsion Elements". Seventh Ed ed. [s.l.] John Wiley & Sons, 2001.

Dos Santos, G. P. "Experimental Evaluation of Hybrid Propulsion Rocket Engine Operating with Paraffin Fuel Grain and Gaseous Oxygen". 2014. 196 f. Tese (Doutorado em Engenharia Aeronáutica e Mecânica) - Instituto Tecnológico de Aeronáutica, São José dos Campos.

Kuo, K. K.; Chiaverini, M. J. "Fundamentals of Hybrid Rocket Combustion and Propulsion". Reston ,VA: American Institute of Aeronautics and Astronautics, 2007.

Kobald, M. et al. "Viscosity and regression rate of liquefying hybrid rocket fuels". Journal of Propulsion and Power, v. 33, n. 5, p. 1245–1251, 2017.

Ito, S.; Kamps, L.; Nagata, H., "Fuel Regression Characteristics in Hybrid Rockets Using $N_2O/HDPE$". Journal of propulsion and power, 37(2), 342-348, 2019.

Marxman, G. and Gilbert, M., "Turbulent Boundary Layer Combustion in the Hybrid Rocket," Symposium (International) on Combustion, Vol. 9, No. 1, 1963, pp. 371-383.

Marxman, G., Wooldridge, C. and Muzzy, R., "Fundamentals of Hybrid Boundary-Layer Combustion," Heterogeneous Combustion, edited by Glassman, I., Green, L. and Wolfhard, H., Vol. 15, Progress in Astronautics and Rocketry, AIAA, 1964, pp. 485-522.

De Zilwa, S. D.; Zilliac, G.; Reinath, M.; Karabeyoglu, A. "Time-Resolved Fuel-Grain Port Diameter Measurement in Hybrid Rockets". Journal of Propulsion and Power, v. 20, n. 4, p. 684-689, 2004.

George, P.; Krishnan, S.; Varkey, P. M.; *et al*. "Fuel Regression Rate in Hydroxyl-Terminated-Polybutadiene/Gaseous-Oxygen Hybrid Rocket Motors". Journal of Propulsion and Power, v. 17, n. 1, p. 35–42, 2001.

Kumar, R.; Ramakrishna, P. A. "Measurement of regression rate in hybrid rocket using combustion chamber pressure". Acta Astronautica, v. 103, p. 226–234, out. 2014.

Chiaverini, M. J. et al. "Regression rate behavior of hybrid rocket solid fuels". Journal of Propulsion and Power, v. 16, n. 1, p. 125–132, 2000.

Evans, B. et al. "Instantaneous Regression Rate Determination of a Cylindrical X-Ray Transparent Hybrid Rocket Motor" American Institute of Aeronautics and Astronautics. July, p. 1–11, 2003.

Sorge, A. R.; Carmicino, C. "Non-Intrusive Regression Rate Measurements in a Hybrid Rocket". 2002.

Osmon, R. V., "Experimental investigation of alithium aluminum hydride-hydrogen peroxide hybrid rocket". Chemical Engineering Progress Symposium, vol. 62, 1966, pp. 92–102.

Wernmont, E.J.; Heister, S.D., "Reconstuction technique for reducing hybrid-rocket combustion test data", J. Propuls. Power15 (1999) 128–136.

Quadros, F. D. A.; Lacava, P. T. "Swirl Injection of Gaseous Oxygen in a Lab- Scale Parrafin Hybrid Rocket Motor Swirl

Injection of Gaseous Oxygen in a Lab-Scale Paraffin Hybrid Rocket Motor". [s.l.] Instituto Tecnológico de Aeronáutica, 2017.

Barros, T. M. "Simulação Experimental do Uso de Parafina como Combustível de Sistema Propulsivo Combinado Motor Foguete a Propelente Híbrido / Ramjet". 2014. 133 f. Dissertação (Mestrado em Engenharia Aeronáutica e Mecânica) – Instituto Tecnológico de Aeronáutica, São José dos Campos.

Dias, I. D. B. "Estudo da Influência da Pós Câmara na Combustão e Desempenho de um Motor Híbrido". 2015. 82 f. Trabalho de Graduação (Curso de Engenharia Aeroespacial) - Instituto Tecnológico de Aeronáutica, São José dos Campos.

Silveira, R. M.; Matos, I. P. B.; Pimont, L. J.; Fernandes, P. C. G. "Validation of the Theoretical Model for Dimensioning the Propellant Characteristics in a Laboratory Scale Hybrid Rocket Motor Bench", 18 th Brazilian Congress of Thermal Sciences and Engineering, 2020.

Olde, M. S., Zandbergen, B. T. C., Jyoti, B. V. S., van den Wijngaart, J. A. B. J., Kuhnert, F. A., van Slingerland, J., "Laser Ignition and Combustion Study of KNO3-Sorbitol based Solid Propellant". Eighth European Conference for Aeronautics and Aerospace Sciences (EUCASS).

Karabeyoglu, A.; Zilliac, G.; Cantwell, B. J.; Dezilwa, S.; Castellucci, P. "Scale-up tests of high regression rate paraffin based hybrid rocket fuels", Journal Propulsion Power 20 (2004) 1037–1045.

Kumar, R.; Ramakrishna, P.A. "Effect of the Protrusion in the Enhancement of Regression Rate in Hybrid Rocket", AIAA Paper 2011–5913.

Gordon, S.; Mcbride, B. J. "Computer Program for Calculation of Complex Chemical Equilibrium Compositions and Applications: I. Analysis". Washington, D.C.: NASA, 1994. 61 p. (NASA RP-1311).

Bianchi, D.; Leccese, G.; Nasuti, F. "Modeling of High Density Polyethylene Regression Rate in the Simulation of Hybrid Rocket Flowfields". 7th European Conference for Aeronautics and Aerospace Sciences (EUCASS). 2017.

Carmicino, C.; Sorge, A. R. "Non-Intrusive Regression Rate Measurements in a Hybrid Rocket". 2005.

Kim, S.; Moon, H.; Kim, J. "Evaluation of Paraffin-Polyethylene Blends as Novel Solid Fuel for Hybrid Rockets". Journal Propulsion Power, 2015.

Gomes, S. R.; Rocco, L.; Rocco, J. A. F. "Swirl Injection Effects on Hybrid Rocket Motors". J. Aerosp. Technol. Manag., São José dos Campos, Vol.7, No 4, pp.418-424, Oct.-Dec., 2015.

De Matos, I. P. B.; Silveira, R. M.; Pimont, L. J.; Gouvêa, L. H.; Lacava, P. T. "Measurement of the Regression Rate in a Hybrid Rocket Motor by Acquiring the Helmholtz Frequency in the Combustion Chamber". 18th Brazilian Congress of Thermal Sciences and Engineering, 2021.

8. RESPONSIBILITY NOTICE

The authors are the only responsible for the printed material included in this paper.